Image Quality and Imaging Depth Analysis of Novel Transmit Schemes with Increased Input Acoustic Energy

Aadavan S
Department of Applied Mechanics
Indian Institute of Technology Madras
Chennai, India
am21s062@smail.iitm.ac.in

Dr Arun Kumar Thittai
Department of Applied Mechanics
Indian Institute of Technology Madras
Chennai, India
akthittai@iitm.ac.in

***Abstract*—Being a safer modality, ultrasound is used in many imaging applications for diagnostic purposes. Adapting novel ultrasound transmit schemes and beamforming techniques are active areas in the field of ultrasound imaging for further improving the image quality. While Conventional Focused Beam (CFB) is an established technique and available commercially, newer synthetic aperture (SA) techniques have shown promise to overcome several limitations of CFB. However, a significant limitation of these SA techniques is that the imaging depth is much less than that of CFB. Although some works employing SA with increased transmit voltage have been shown to overcome the imaging depth challenge, not much work is reported on their thermal and mechanical indices (TI and MI), which is of prime importance to estimate the safety of ultrasound exposure. This work attempts to analyze and compare the image quality and imaging depth improvements for the different SA schemes for increased input acoustic energy while keeping the MI and TI below that of CFB. Specifically, Synthetic Transmit Aperture (STA) and Diverging Beam with Synthetic Aperture Technique (DB-SAT) are compared with CFB. Contrast ratio (CR) and Contrast to Noise Ratio (CNR) parameters are taken for image quality analysis. The experiments using needle hydrophone were done. The maximum allowable limits for MI and TI values for CFB were taken from IEC 62359 standard report. The result suggests that an additional increase in input voltage to STA and DB-SAT schemes yielded an improvement in contrast ratio and imaging depth, without crossing the safety threshold. Thus, by carefully adopting a higher input voltage for the synthetic aperture schemes, one could be within safe limits of TI and MI and still improve the imaging depth.**

Keywords—ultrasound imaging, ultrasound safety exposure, CFB, STA, DB-SAT, Mechanical Index (MI), Thermal Index (TI), needle hydrophone

I. INTRODUCTION

Medical ultrasound imaging is a ubiquitous modality where conventional focused beamforming (CFB) technique is commonly utilized [1]. This technique is known to provide better quality images at the focus, and its safety is assessed by estimating mechanical index (MI) and thermal index (TI). One of the major limitations of CFB is that the image quality deteriorates beyond the focus, and a tighter focus requires a larger active aperture. One common way to overcome this limitation, especially for large imaging depths, is to employ multiple foci during transmission. However, the frame rate reduces with multiple transmit foci. Thus, the cost and complexity of ultrasound scanners are known to scale up with image quality in CFB.

Several other transmit beamforming techniques have also been investigated to address some of these tradeoffs with CFB. For example, in Synthetic Transmit Aperture (STA) scheme, a single element is excited at a time to transmit an unfocused wave and dynamic focusing is employed on the received echoes [2]. Although this technique gives depth-independent lateral resolution, it suffers from limited imaging depth due to only one element serving as an active aperture at a time.

The concept of diverging beam in combination with synthetic aperture (DB-SAT) has been reported to provide better quality images at higher frame rates than possible with CFB scheme [3]. Here, the source is considered to be placed behind the transducer, creating a virtual source. When excited, this creates a diverging beam during transmission. However, the imaging depth is smaller than that of CFB. Clearly, the acoustic energy experienced by the tissues varies depending on the transmit schemes, which dictates the imaging depth. However, transmitting high energy may cause either mechanical or thermal damage to the soft tissue [4], [5]. The estimates of safety indices have been extensively analyzed and reported for CFB [6], which sends out the most energy and hence yields superior imaging depth compared to the synthetic aperture techniques described in the previous paragraphs. Certain SA techniques with Hadamard encoded signals are done for SNR and resolution enhancement for which the safety indices are estimated [7].

In summary, not much research has been published on improving imaging depth by increasing the input acoustic energy through the limited active transmit elements for the synthetic aperture schemes. Therefore, investigating this aspect, while staying within the safety levels of CFB, forms the objective of the current work reported here.

II. MATERIALS AND METHODS

A. Experiments with needle hydrophone

Figure 1 shows a block diagram of the experimental setup comprising a needle hydrophone in a water tank to measure the acoustic pressure output from the ultrasound array transducer when excited with an input voltage. The pressure wave from the transducer travelling through water was measured using a 0.2mm needle hydrophone (Precision Acoustics, UK). The DC coupler acted as an acoustic signal coupler between the needle hydrophone and oscilloscope (DSOX1102G, Keysight, USA).

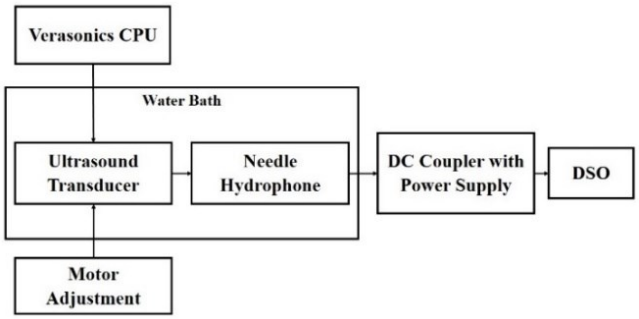

Fig. 1: Block diagram of the experimental setup used to capture the transducer output as voltage waveform using needle hydrophone.

A stepper motor control was used to move the transducer along the X, Y and Z axes using Repetier® Host software (V2.2.4, Hot-World GmbH & Co. KG, Germany) to measure the output at different spatial locations. The voltage amplitude output of the hydrophone was converted to pressure value by dividing it with the calibrated sensitivity of the hydrophone (from the manufacturer data sheet, it was 59 mV/MPa at 7.5 MHz operating frequency) as pressure component was the parameter of interest to estimate the safety indices MI, TI using formulae (1), (2) respectively

MI	TI
$\frac{p_{r,\alpha}(z_{MI})f_{a\omega f}^{-1/2}}{C_{MI}}$ (1)	$min\left(\frac{W(z).f_{awf}}{210\ mW\ MHz}, \frac{I_{spta}(z).f_{awf}}{210\ mW\ MHz\ cm^{-2}}\right)$ (2)

where, f_{awf} is acoustic working frequency, $p_{r,\alpha}$ is rarefactional pressure amplitude after attenuation and C_{MI} = 1MPa/MHz$^{1/2}$. W and I_{spta} are calculated using the formulae (3), (4) respectively

W	I_{spta}
$\frac{(z\lambda p_{r,\alpha})^2}{A\rho c}$ (3)	$\frac{(p_{r,\alpha})^2}{\rho c}$ (4)

where, z is the depth, λ is the wavelength, A is the transducer aperture area, ρ is the density and c is the speed of sound in propagation medium [6],[8],[9] ,[10].

B. Transmit schemes and beamforming

CFB, STA and DB-SAT transmit schemes were implemented in Verasonics-64 system (Verasonics Inc., Redmond, WA, USA) using the linear probe **L11-5**. The relevant transducer parameters are listed in Table 1.

TABLE 1: Transducer parameters used for experiment.

Parameters	Values
Number of elements	128
Inter element spacing	0.3 mm
Element width	1.3 mm
Center frequency	7.5 MHz
Sampling frequency	31.25 MHz

Active transmit aperture consisted of 64, 1 and 8 elements for CFB, STA and DB-SAT, respectively. The received RF data was beamformed using delay and sum (DAS) technique, envelope detected and log compressed to form an image [10]. To compare the contrast among different schemes, experiments were done on a commercially available tissue mimicking phantom (CIRS Model 040GSE, USA) and the contrast ratio (CR), contrast to noise ratio (CNR) were estimated [3],[12] using the formulae (5), (6) respectively

CR	CNR
$\frac{(s_{out}-s_{in})}{s_{out}}$ (5)	$\frac{20\ log_{10}\lvert s_{out}-s_{in}\rvert}{\sqrt{\sigma_{in}^2-\sigma_{out}^2}}$ (6)

where, s_{out} and s_{in} are mean intensity values, σ_{out} and σ_{in} are the corresponding standard deviations of target and background respectively.

III. RESULTS AND DISCUSSION

As per the IEC 62359 standards recommendation, ultrasound transducer can be operated within a maximum allowable limit of 1.9 for MI and 6 for TI. In order to prevent transducer damage, we placed a hard limit of 50V on the input excitation voltage. Therefore, without losing the generality of our objective, it was sufficient to operate the SA schemes at input voltage of 50V and the same schemes along with CFB at a lower applied voltage for this comparative analysis

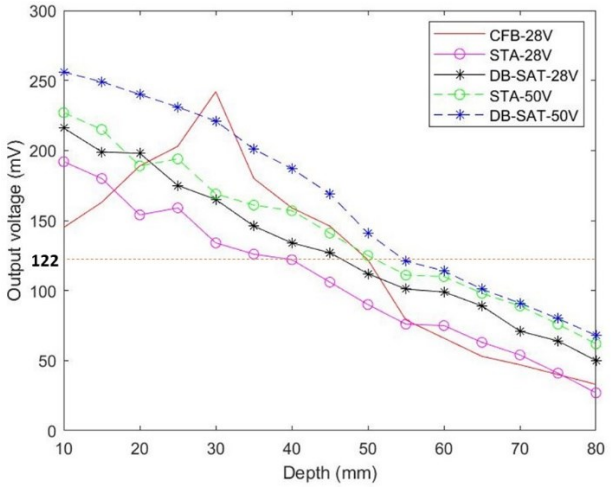

Fig. 2: Plot showing output voltages measured using needle hydrophone at different depths for CFB, STA and DB-SAT transmit schemes.

Figure 2 shows the comparison of recorded output voltages from the needle hydrophone for CFB, STA and DB-SAT schemes. Here, CFB scheme is implemented having the focus at 30 mm depth and the virtual source is taken at 1.2 mm behind the transducer for the DB-SAT scheme. The hydrophone voltage was measured along the center axis of the beam pattern. The measurement was taken at a distance of 10 mm from the transducer surface and continued till 80 mm along the depth. Initially, all the three schemes were operated at an input voltage of 28V. Subsequently, the input voltage to the transducer was increased to 50V only for STA and DB-SAT schemes and the respective output voltage was plotted.

It is clear from Figure 2 that for the same applied input voltage (=28V), CFB has better signal strength in the transmitted wave at the focus (=30mm) and slightly beyond. Also, it is observed that the signal strength in CFB drops drastically after 52mm. Hence, the output voltage of 122mV at 52mm depth can be considered as the minimum sufficient signal strength for imaging. Taking this as a reference, and if we analyse the imaging depth, this comes out to be 52 mm, 40 mm and 45 mm for CFB, STA and DB-SAT schemes, respectively. However, when the operating input voltage is increased to 50V for STA and DB-SAT, the imaging depth is increased to 50 mm and 55 mm, respectively.

TABLE 2: Calculated MI and TI values for CFB, STA and DB-SAT transmit schemes operated at different input voltages.

	CFB @28V	**STA @28V**	**STA @50V**	**DB-SAT @28V**	**DB-SAT @50V**
MI	**0.386**	0.348	**0.369**	0.371	**0.397**
TI	**1.653**	1.399	**1.535**	1.563	**1.698**

Table 2 lists the MI and TI values for the transmit schemes at different input voltages, calculated using (1) and (2). It can be observed that the MI and TI values are almost equal, and under the maximum allowable limit, for CFB operated at 28V and STA, DB-SAT at 50V. Hence, in this case, the image quality and imaging depth can be compared.

Figure 3 (a) shows image of the reference cross sectional view of CIRS phantom having hypoechoic cysts at depth 14mm, 29mm and 43 mm that was imaged using ultrasound. Figure 3 (b), (c), (d), (e) and (f) show the B mode images reconstructed using DAS for different transmit schemes. It can be observed from Figure 3 that the imaging depth is increased (as cyst at 43mm is visible in STA and DB-SAT schemes) in synthetic aperture techniques with increased input voltage, and the imaging depth is almost comparable to that of CFB. This corroborates the expectation of increased imaging depth in SA techniques when operated at increased input voltage. Also, the image contrast obtained using DB-SAT scheme operated at 50V is comparable to the contrast obtained using CFB scheme operated at 28V. The Contrast Ratio (CR) and Contrast to Noise Ratio (CNR) from the images obtained using the different operationg conditions is listed in table 3.

TABLE 3: Calculated CR and CNR values for the images obtained using different transmit schemes

	CFB	**STA @50V**	**DB-SAT @50V**
CR	0.9586	0.9477	0.9513
CNR (dB)	15.5318	14.678	14.775

The CR and CNR values are estimated using the formulae (5) and (6) by taking the cyst target at a depth of 30 mm from the transducer surface, marked by a yellow rectangular window shown in Figure 3(f).

IV. CONCLUSION

The idea of overcoming the limitation of imaging depth in SA techniques by operating with higher input voltage was implemented in this work. The measured signal strength value at different depths suggests that the imaging depth can be increased for the SA techniques by increasing the input voltage, while still remaining within the limits prescribed for MI and TI in CFB.

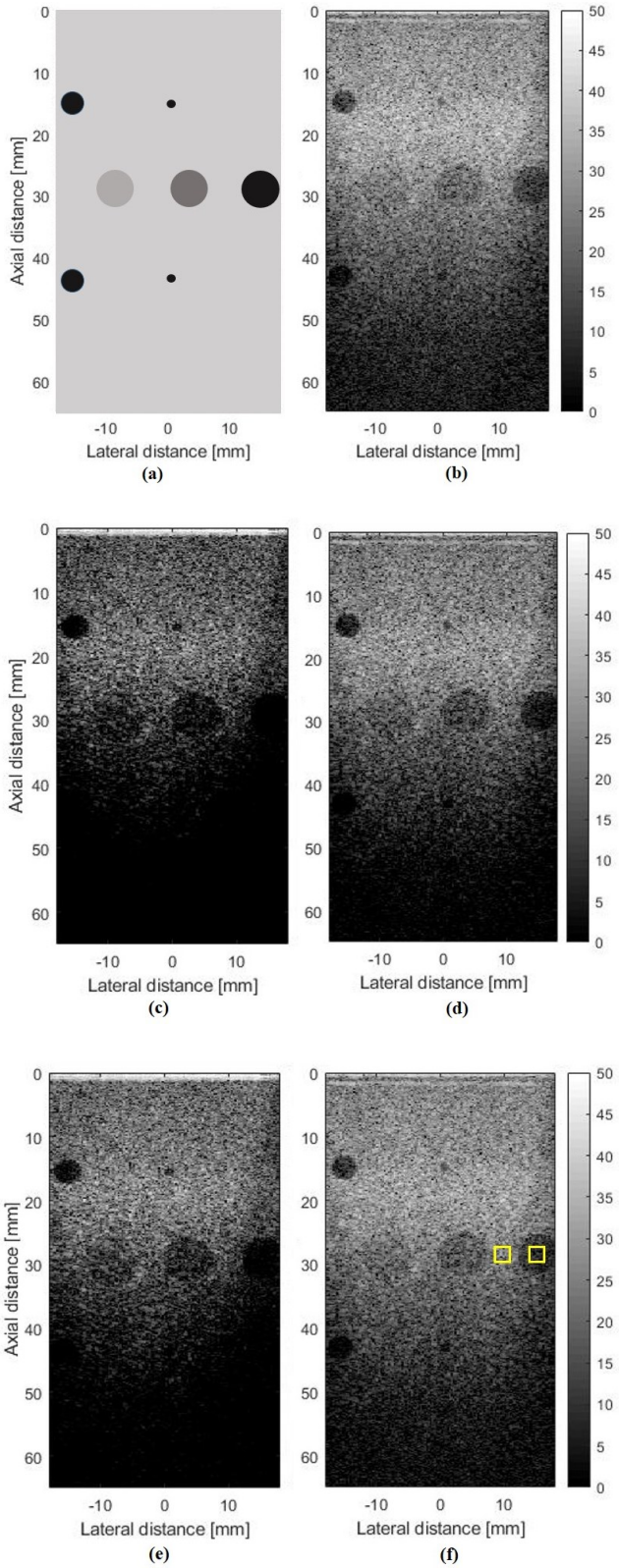

Fig. 3: Images of (a) cross sectional view of CIRS phantom used for experiments and its corresponding B mode image obtained using (b) CFB 28V, (c) STA 28V, (d) STA 50V, (e) DB-SAT 28V and (f) DB-SAT 50V schemes

Further, it is also shown that the SA techniques have image quality, in terms of CR and CNR, which is comparable with those obtained by employing the CFB scheme operated at reference input voltage. However, a more thorough statistical analysis of these data will pave the way for an effective comparison assessment, which is intended to be a follow-up to this work.

ACKNOWLEDGMENT

The student author, Aadavan S, would like to thank the Ministry of Human Resource Development (MHRD), Government of India, for the financial support through stipend.

REFERENCES

[1] Cobbold, R. S. Foundations of biomedical ultrasound. Oxford university press. (2006).

[2] Ihor TROTS, Andrzej Nowicki, Marcin Lewandowski, "Synthetic Transmit Aperture in Ultrasound Imaging", Archives of Acoustics, **34**, 4, pp. 685-695 (2009).

[3] B. Lokesh, Arun K. Thittai, "Diverging beam transmit through limited aperture:A method to reduce ultrasound system complexity and yet obtain better image quality at higher frame rates", Ultrasonics, Pages 150-160 (2019).

[4] Marhenke, Torben, Sergio J. Sanabria, Bhaskara Rao Chintada, Roman Furrer, Jürg Neuenschwander, and Orcun Goksel. "Acoustic field characterization of medical array transducers based on unfocused transmits and single-plane hydrophone measurements." *Sensors* 19, no. 4 (2019): 863.

[5] C. Kollmann, G. ter Haar, L. Dolezal, M. Hennerici, K. A. Salvesen, Lil Valentin, "Ultrasound Output : Thermal (TI) and Mechanical (MI) Indices", ultraschall in der Medizin, vol 34, pp 422-434 (2013).

[6] Jingfeng Bai, Xiumei Huang, Lu Xie, Yazhu Chen, "Acoustic Field Measurement and Analysis for a Spherical Phased Array by PVDF Needle Hydrophone", IEEE (2009).

[7] P. Gong, P. Song and S. Chen, "Ultrafast Synthetic Transmit Aperture Imaging Using Hadamard-Encoded Virtual Sources With Overlapping Sub-Apertures," in IEEE Transactions on Medical Imaging, vol. 36, no. 6, pp. 1372-1381, (2017).

[8] Keith A. Wear, "Hydrophone Spatial Averaging Correction for Acoustic Exposure Measurements from Arrays-Part I: Theory and Impact on Diagnostic Safety Indexes." IEEE Transactions on Ultrasonics, Ferroelectrics, And Frequency Control, Vol. 68, No. 3 (2021).

[9] Keith A. Wear, Aoife M "Hydrophone Spatial Averaging Correction for Acoustic Exposure Measurements from Arrays-Part II: Validation for ARFI and Pulsed Doppler Waveforms." IEEE Transactions on Ultrasonics, Ferroelectrics, And Frequency Control, Vol. 68, No. 3 (2021).

[10] Jørgen Arendt Jensen, et al, "Safety Assessment of Advanced Imaging Sequences I: Measurements", IEEE Transactions On Ultrasonics, Ferroelectrics, And Frequency Control, vol. 63, no. 1, (2016).

[11] Thomenius, K. E. Evolution of ultrasound beamformers. In 1996 IEEE Ultrasonics Symposium. Proceedings (Vol. 2, pp. 1615-1622). IEEE. (1996).

[12] Hideyuki Hasegawa, "Advances in ultrasonography: image formation and quality assessment", Journal of Medical Ultrasonics 48:377–389 (2021).